DOI 10.5162/Ultrasonic2025/C13-c1

Inversion of the corrugation parameters of a double corrugated liquid/solid interface from the diffraction of homogeneous plane waves with the Ultrasonic Polar Scan

Emil Aleksiewicz-Drab[1], Mathias Kersemans[2,3], and Koen Van Den Abeele[1]
[1]KU Leuven Campus Kulak, Dept. of Physics, Belgium
[2] Ghent University, Dept. of Materials, Textiles and Chemical Eng., Ghent, Belgium
[3]Flanders Make, FlandersMake@UGent, Corelab MIRO, Lommel, Belgium
emil.aleksiewicz-drab@kuleuven.be

Abstract: This study focuses on inverting the geometrical characteristics of the surface of corrugated interfaces from ultrasonic polar scan data. Based on an analytical model to predict the reflection and transmission of homogeneous plane waves on a 2D periodically corrugated surface, and in combination with numerical calculations and machine learning, we were able to inversely estimate the corrugation parameters (the periodicity, shape and height) from the reflected ultrasonic polar scan landscape.

Keywords: Ultrasonic Polar Scan, Periodically corrugated surface, Corrugation height, Non-destructive characterization, 2-D corrugated surface.

Introduction

In the past, several studies of acoustic waves interacting with corrugated materials have been reported, for both 1-D [1–5] and 2-D [6] surface corrugations due to its potential use in material characterization and non-destructive testing (NDT). These studies investigated the interaction of homogeneous as well as inhomogeneous plane waves, and showed that the geometrical parameters which describe the corrugation, such as the corrugation period Λ, the height h and the shape S, significantly influence the scattering characteristics of particular modes in reflection or transmission [3].On the other hand, to our knowledge, only one study so far has been dedicated to the inverse estimation of the underlying interface properties themselves [7]. This experimental work, be it quite limited, showed interesting potential for further exploration of the inverse problem with the help of theoretical models as a guideline for the inversion of the corrugation characteristics. In addition, ongoing development of a novel phased array (PA)-based Ultrasonic Polar Scan (UPS) [8–10] device should be able to facilitate a more comprehensive means for accelerated experimental measurements and verification.

In the current paper, we first reintroduce the state-of-the-art theoretical framework. Next, we show how specific corrugation parameters can be estimated using numerical calculation and machine learning, keeping in mind the possibilities and limitations of future experimental validation. Finally, we discuss the inversion results and the validity of this approach, which points to potential limitations and the need for a next generation experimental measurement campaign.

Mathematical framework for the forward model

We consider a doubly corrugated surface at a single liquid-solid boundary given by:

$$g(x,y,z) = f(x,y) - z = f_x(x) + f_y(y) - z = 0 \quad (1)$$

with

$$f_x\left(x+\Lambda_x\right) = f_x(x),\ f_y\left(y+\Lambda_y\right) = f_y(y) \quad (2)$$

An incident homogeneous plane wave $\mathbf{N}^{inc}$, with a complex wave vector $\mathbf{k}^{inc}$, interacts with the corrugated interface and is scattered into multiple wave fields in reflection and transmission. The wavefield contributions of the incident wave (*inc*), the reflected longitudinal in the liquid (*r*), and the transmitted dilatational (*d*) and shear components (s) in the solid), representing the solutions to the time-independent wave equation as infinite series, can be written as

$$N^{inc} = A^{inc}\phi^{inc}(ik_x^{inc}e_x + ik_y^{inc}e_y + ik_z^{inc}e_z) \quad (3)$$

$$N^r = \sum_{m,n} R^{m,n}\phi^{m,n,r}\left(ik_x^{m,n,r}e_x + ik_y^{m,n,r}e_y + ik_z^{m,n,r}e_z\right) \quad (4)$$

$$N^d = \sum_{m,n} A^{m,n,d}\phi^{m,n,d}\left(ik_x^{m,n,d}e_x + ik_y^{m,n,d}e_y + ik_z^{m,n,d}e_z\right) \quad (5)$$

$$N^s = \sum_{m,n} A^{m,n,s}\phi^{m,n,s}P^{m,n,s} \quad (6)$$

with A^{inc} the amplitude of the incident wave, and $R^{m,n}$, $A^{m,n,d}$, $A^{m,n,s}$ the complex valued amplitudes of the reflected longitudinal, transmitted dilatational and transmitted shear of order m, n respectively, which are directly proportional to A^{inc}. Further, the acoustic potentials can be expressed as $\phi^{\zeta} = e^{i(k^{\zeta} \cdot r)}$ for $\zeta \in \{(m,n,r);\ (m,n,d);\ (m,n,s)\}$, and

$$k_x^{m,n,s} P_x^{m,n,s}, k_y^{m,n,s} P_y^{m,n,s} + k_z^{m,n,s} P_z^{m,n,s} = 0 \tag{7}$$

where $\mathbf{P}^{m,n,s}$ is the polarization vector.

The displacement components Eq. (3) – Eq. (6) have to obey the continuity conditions at the boundary $z = f(x,y)$[11], consisting of the continuity of the normal displacement across the interface:

$$\begin{aligned} \left(N^{inc} + N^{r}\right) \cdot \nabla g = \left(N^{d} + N^{s}\right) \cdot \nabla g \\ \text{on } g(x,y,z) = 0 \end{aligned} \tag{8}$$

and the continuity of the normal and tangential stresses below (1) and above (2) the boundary

$$\sum_j T_{ij}^1 (\nabla g)_j = \sum_j T_{ij}^2 (\nabla g)_j,\ i,j = x,y,z \tag{9}$$

$$\begin{aligned} \left(A_{mn}^s P_x^{m,n,s} k_x^{m,n,s} + A_{mn}^s P_y^{m,n,s} k_y^{m,n,s} \right. \\ \left. + A_{mn}^s P_z^{m,n,s} k_z^{m,n,s}\right) \phi^{m,n,s} = 0 \end{aligned} \tag{10}$$

The established conditions Eq. (8) – Eq. (10) lead to five equations that are periodic in x and y, where a sufficient condition for the solution is to demand that the Fourier coefficients are equal over the intervals $[0,\ \Lambda_x] \times [0,\ \Lambda_y]$, resulting in a linear system of equations in the unknown coefficients $R^{m,n}$, $A^{m,n,d}$, $A^{m,n,s}$. The whole system is however too large to enclose in this paper. Included in the system are wavenumbers, $k_\gamma^\eta = k_\gamma^{inc} + \eta \frac{2\pi}{\Lambda_\gamma}$ with $\eta \in \{m,n\}$ and $\gamma \in \{x,y\}$, denoting the wave-vector components in the γ direction of the η-th order scattered waves which are projected on the surface, and which obey the generalized Snell's law for periodic gratings [6].

Note that this quasi-analytical description of the scattered ultrasonic field is only valid for small roughness [12], i.e. $\Lambda_x, \Lambda_y \approx \lambda$ and $h \ll \lambda$, where λ is the wavelength of the incident wave, and h is the height of the corrugation.

Numerical calculations

Although the linear system of equations is infinite by construction, the infinite summation may be truncated based on an intuitively decreasing amplitude with mode number. Assuming a maximum mode value N_γ, the dimension of the linear system to be solved is (5 (2N_x+1) (2N_y+1) by 5 (2N_x+1) (2N_y+1)).

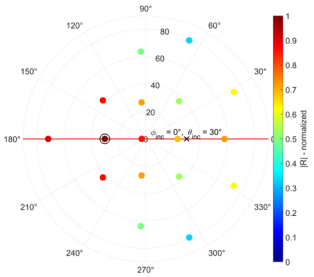

(a) $h = 50\,\mu m, \quad \Lambda = 1.1\,mm$

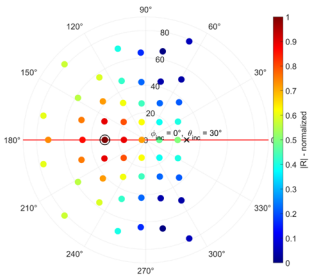

(b) $h = 100\,\mu m, \quad \Lambda = 2.2\,mm$

Fig. 1: Reflection landscape in a polar plot representation for two different corrugation periodicities Λ and two different corrugation heights h

Throughout this paper, a symmetric doubly corrugated surface between water and brass will be considered, and $N_x = N_y = 4$ is taken for both scattering directions. Further, we assume: density $\rho_w = 1000\ \mathrm{kg/m^3}$ for water and $\rho_b = 8100\ \mathrm{kg/m^3}$ for brass; dilatational wave speed $v_w = 1480\ \mathrm{m/s}$ for water and $v_{bd} = 4840\ \mathrm{m/s}$ for brass; shear wave speed for brass is $v_{bs} = 2270\ \mathrm{m/s}$. ; attenuation $\alpha_{wd}\omega^2 = 4 \times 10^{-8}\ \frac{\mathrm{Np}}{\mathrm{mm}}$ at $1\,\mathrm{MHz}$ for water, while $\alpha_{bd}\omega^2 = 4 \times 10^{-6}\ \frac{\mathrm{Np}}{\mathrm{mm}}$ and $\alpha_{bs}\omega^2 = 2 \times 10^{-5}\ \frac{\mathrm{Np}}{\mathrm{mm}}$ at $1\,\mathrm{MHz}$ for brass. In terms of 2D corrugation, we consider three basic shapes: a sinusoidal corrugation, a triangular corrugation and a square corrugation. As an example, Fig. 1 shows the reflection landscape in a polar plot representation for an homogeneous incident plane wave at $\Psi^{inc} = \left[\theta^{inc} = 30°,\ \varphi^{inc} = 0°\right]$ from a 2D sawtooth corrugated interface between water and brass for different corrugation periodicities and different heights. The dots represent the polar position of the modes in reflection, while the colour of the dots is linked to the mode's amplitude.

Inverse estimation of corrugation characteristics

For practical NDT applications, the ultimate goal is to estimate the values of the corrugation parameters Λ_x, Λ_y, h, S from observable experimental data,

i.e. while having access only to the reflection angles for different modes, being a combination of θ_r^{mn} and φ_r^{mn}, and the magnitude of the reflection coefficient $R^{m,n}$ of these modes as input values to perform the inversion. Calculation of Λ_x, Λ_y is relatively simple and comes from Snell's law for periodic gratings [6].

$$k_x^m = k_x^{inc} + m\frac{2\pi}{\Lambda_x},\ k_y^n = k_y^{inc} + n\frac{2\pi}{\Lambda_y} \tag{11}$$

These equations allow to express the angles of the reflected mode '*m,n*' as a combination of a polar φ_r^{mn} and reflection θ_r^{mn} angle in the following way:

$$\varphi_r^{mn} = \tan^{-1}\left(\frac{k^{inc}\sin\theta^{inc}\sin\varphi^{inc} + n\frac{2\pi}{\Lambda_y}}{k^{inc}\sin\theta^{inc}\cos\varphi^{inc} + m\frac{2\pi}{\Lambda_x}}\right) \tag{12}$$

$$\theta_r^{mn} = \sin^{-1}\left(\frac{1}{k_r^{mn}}\sqrt{\begin{aligned}&\left(k^{inc}\sin\theta^{inc}\right)^2 \\ &+4\pi k^{inc}\sin\theta^{inc} \\ &\times\left(\frac{m}{\Lambda_x}\cos\varphi^{inc} + \frac{n}{\Lambda_y}\sin\varphi^{inc}\right) \\ &+4\pi^2\left(\left(\frac{m}{\Lambda_x}\right)^2 + \left(\frac{n}{\Lambda_y}\right)^2\right)\end{aligned}}\right) \tag{13}$$

Assuming $\theta^{inc} = 0$, corresponding to normal incidence, those expressions can be largely simplified, and lead, after straightforward calculations, to potential expressions for the corrugation periods Λ_x and Λ_y;

$$\Lambda_y = \left|\frac{2\pi n\sqrt{1+\tan^2\varphi_r^{mn}}}{k_r^{mn}\sin\theta_r^{mn}\tan\varphi_r^{mn}}\right|,\ \Lambda_x = \left|\frac{m\Lambda_y\tan\varphi_r^{mn}}{n}\right| \tag{14}$$

Thanks to the fact that the new UPS device that we intend to develop in the future using phased array technology will be able to gather reflected signals at multiple angles at once, one experimental measurement at one incidence angle should in theory be sufficient to determine both lengths.

The inversion of the corrugation height h and the shape S is far more complicated, because there is no a-priori simple relation to the input parameters $R^{m,n}$. Since the forward model is computationally inexpensive, a data-driven approach is proposed to estimate these two parameters. The database was created by varying the input parameters θ^{inc}, φ^{inc}, f, h, S, resulting in nearly 3.5 million unique combination, for which a set of reflection coefficients was obtained. The proposed inversion approach is a two-step method, where first the shape S is determined, followed by an estimation of the corrugation height h. This approach is a result of preliminary testing which showed that knowing the shape beforehand massively improves the accuracy of the height estimation. Both approaches rely on supervised machine learning but use different techniques.

For the shape estimation, we considered four different shapes: two variations of a rectangular corrugation with a duty cycle of 90% (S_{R90}) and 75% (S_{R75}) respectively, a symmetrical triangular corrugation(S_T) and a sinusoidal corrugation(S_S). Wide Neural Network was used in this classifier [13, 14], with 100 neurons fully connected to the first layer. The costs of misclassification were set to 0 when the predicted shape matches the true one, and 1 otherwise. The data was split into 80/20 for training/validation and testing. The predictors were provided in the following form: $(\theta^{inc},\ \varphi^{inc},\ |R^{m,n}(f)|)$, where $m, n \in \{-1, 0, 1\}$ and f being 25 different frequencies ranging from 500 kHz to 2.5 MHz, essentially meaning that we provide the values of the first nine modes of the reflection coefficient as a function of frequency, on a grid of polar and azimuthal incident angles. Even though the height h is also varied between 10 to 90 μm in the database, it is not provided as one of the predictors, since in an experimental setting with an unknown sample, this parameter would a priori be unknown. Because the model is trained with purely synthetic data, k-fold cross validation was used to ensure some degree of robustness, as well as 5% Gaussian noise to all of the $R^{m,n}$ modes used, simulating a realistic measurement uncertainty in an experimental condition. The performance of the classifier is presented in Fig. 2 in the form of a confusion matrix which shows the correctness of the assignments in terms of percentages for each shape. The labels from 1 to 4 correspond to S_{R90}, S_{R75}, S_T and S_S respectively.

While the average accuracy of the model is 93%, the quality of the assignments is different for S_{R90} and S_S when compared to S_{R75} and S_T, with the former being significantly better, which can be attributed to the fact that these modes are more distinguishable when compared to the other two based on the features for classification used here. The addition of noise heavily impacted the accuracy of the model, as the tests without it showed a performance of 99.5% instead.

The performance of the classifier was then propagated further into a regression model used to estimate the height. The regression model was a bagged decision tree ensemble [15]. This method combines multiple decision trees to improve prediction accuracy and reduce overfitting. The model was structured in such a way, that the minimum leaf size was 5, with 40 learners in total. The input array for the predictors

DOI 10.5162/Ultrasonic2025/C13-c1

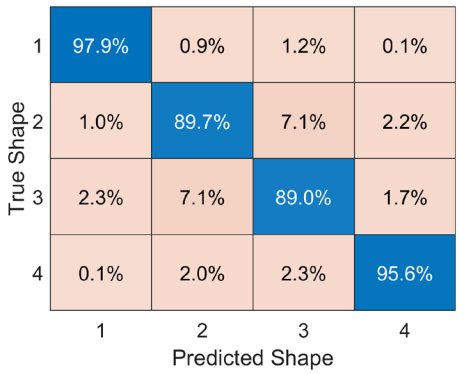

Fig. 2: Confusion matrix for 4 different shapes obtained after testing the neural network model.

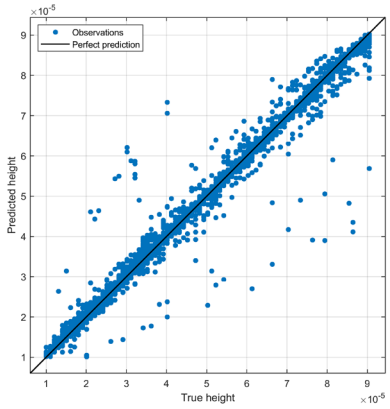

Fig. 3: Predicted vs true height plot obtained using the bagged tree ensemble model.

was almost the same as in the case of the classifier, however the shapes are now assumed to be known along with the classifier's performance.

To incorporate that information, each of the shapes was weighted using the probability distribution obtained from the confusion matrix, e.g. for S_S 95.6% of the inputs were labelled as S_s, 0.1% as S_{R90}, 2% as S_{R75} and 2.3% as S_T respectively. To avoid the model being overly optimistic, 25 frequencies were used for the predictors which were different than the ones used for the classifier. The performance of the model was assessed using common metrics and a 'predicted vs actual' plot is shown in Fig. 3, where the blue dots represent individual estimated height values, and the black straight line denotes the perfect prediction.

The Mean Average Error (MAE) is $0.789\ \mu m$, whereas the Root Meas Square Error (RMSE) is $2.51\ \mu m$. This means that, while the average error is relatively small taking into account the range of corrugation heights used for training, there are large outliers as indicated by the RMSE, which can most probably be attributed to a misclassification of the shapes in the earlier stage. This also implies that the shape influences the value of $|R^{m,n}|$ independently of the height.

Concluding remarks

A hybrid analytical-numerical model to study the impact of different geometries of doubly periodic corrugated interfaces on the reflection landscape of an incident ultrasonic plane wave was used as the basis to develop methods allowing an estimation of the corrugation parameters: the corrugation period Λ, the height h and the shape S. Using a data-driven machine learning approach, it was shown that for relatively small h, it is possible to estimate these geometric parameters for an unknown sample. Although the precision to which this method is able to estimate the height is lower than a regular profilometer, it can still provide globally useful information for some applications. Despite the method's inherent limitations, it can serve as a good starting point for further research. Firstly, the procedure should be validated with a series of experiments. This could be performed as part of a novel use-case for a new UPS design with phased array emission and reception in reflection, which is currently under development. In addition, an extension to a plate corrugated on one/two sides can be considered and studied in detail to eventually define inversion strategies in a similar way as was suggested in this paper.

Acknowledgements

Research funded by the KUL C2 project [C24_21_22].

References

[1] Mampaert and Leroy. J. Acoustical Society of America, 83(4):pp. 1390–1398.
[2] Claeys et al. Journal of Applied Physics, 54(10):pp. 5657–5662.
[3] V. D. Abeele. et al. J. Acoustical Society of America, 99(5):pp. 2883–2897.
[4] Briers and Leroy. SPIE, 1844:pp. 196–205.
[5] Briers et al. J. Acoustical Society of America, 106(2):pp. 682–687.
[6] Declercq. et al. Ultrasonics, 43(8):pp. 605–618.
[7] Liu and Declercq. Ultrscs, 53(4):pp. 853–861.
[8] Daemen. PhD Thesis KU Lueven. 2020.
[9] Martens. PhD Thesis KU Lueven. 2020.
[10] Kersemans. PhD Thesis UGent. 2014.
[11] Charlier and Crowet. J Acoust Soc Am, 79(4):pp. 895–900.
[12] Lippmann. JOSA, 43(5):pp. 408–408.
[13] Radhakrishnan et al. Proc of the National Academy of Sciences, 120(14).
[14] Anders and Korn. Neural Networks, 12(2):pp. 309–323.
[15] Breiman. Mach Learn, 24(2):pp. 123–140.